Collective quantization of axially symmetric gravitating $B = 2$ skyrmion

Hisayuki Sato,[1,*] Nobuyuki Sawado,[1,†] and Noriko Shiiki[1,2,‡]

[1]*Department of Physics, Faculty of Science and Technology, Tokyo University of Science, Noda, Chiba 278-8510, Japan*
[2]*Department of Management, Atomi University, Niiza, Saitama 352-8501, Japan*
(Received 27 September 2006; published 12 January 2007)

In this paper we perform collective quantization of an axially symmetric skyrmion with baryon number two. The rotational and isorotational modes are quantized to obtain the static properties of a deuteron and other dibaryonic objects such as masses, charge densities, and magnetic moments. We discuss how gravity affects those observables.

DOI: 10.1103/PhysRevD.75.014011 PACS numbers: 12.39.Dc, 04.20.−q, 21.10.−k

I. INTRODUCTION

The Skyrme model [1] is considered an unified theory of hadrons by incorporating baryons as topological solitons of pion fields, called skyrmions. The topological charge is identified as the baryon number B. Performing collective quantization for a $B = 1$ skyrmion, one can obtain proton and neutron states within 30% error [2].

Correspondingly, multiskyrmion solutions are expected to represent nuclei [3–5]. The static properties of a $B = 2$ skyrmion such as mass spectra, mean charge radius, baryon number density, magnetic moment, quadrupole moment, and transition moment were studied in detail by Braaten and Carson upon collective zero-mode quantization [6]. The results confirmed that the quantized $B = 2$ skyrmion can be interpreted as a deuteron.

The Einstein-Skyrme model in which the Skyrme fields coupled to gravity was first considered by Luckock and Moss [7]. They obtained spherically symmetric black hole solutions with Skyrme hair. It is the first discovered counter example to the no-hair conjecture. Axially symmetric regular and black hole skyrmion solutions with $B = 2$ were constructed in [8]. Subsequently the model was extended to the $SU(3)$ and higher baryon number with discrete symmetries to study gravitating skyrmion solutions [9].

In the Einstein-Skyrme theory, the Planck mass is related to the pion decay constant f_π and coupling constant α by $M_{\rm pl} = f_\pi\sqrt{4\pi/\alpha}$. To realize the realistic value of the Planck mass, the coupling constant should be extremely small with $\alpha \sim O(10^{-39})$, which makes the effects of gravity on the skyrmion negligible. We, therefore, consider α as a free parameter and study the strong coupling limit to manifest the effects of gravity on skyrmion spectra. The property of the skyrmion solution could be drastically changed for large values of α. Certainly studying the effects of gravity on soliton spectra is interesting itself. Nevertheless, we further attempt to give an interpretation to the solution as a gravitating deuteron or dibaryonic object and study their mass spectra and other static observables.

The first step towards the study of gravitational effects on the quantum spectra of skyrmions was taken in Ref. [10] by performing collective quantization of a $B = 1$ gravitating skyrmion. It was shown there that the qualitative change in the mass difference, mean charge radius, and charge densities under the strong gravitational influence confirms the attractive feature of gravity while the reduction of the axial coupling and transition moments by the strong gravity indicates the gravitational effects as a stabilizer of baryons.

In this paper we extend the work [10] to the $B = 2$ axially symmetric gravitating skyrmion and estimate the static properties of a deuteron or other dibaryonic objects. We observe how strong gravity affects the baryon observables e.g., mass spectra, mean charge radius, baryon number density, magnetic moment, quadrupole moment, and transition moment.

Although the Skyrme model describes nucleons with about 30% error, the possibility that it may provide qualitatively correct description of the interaction of baryons with gravity cannot be excluded. It is expected that in the early universe or equivalent high energy experiments, the gravitational interaction with baryons is not negligible. We hope that our work could provide insight into the observations in such situations.

II. CLASSICAL GRAVITATING $B = 2$ SKYRMIONS

In this section, we discuss $B = 2$ classical regular solutions in the Einstein-Skyrme system. The Skyrme Lagrangian coupled to gravity is defined by the Lagrangian

$$\mathcal{L} = \mathcal{L}_G + \mathcal{L}_S, \tag{1}$$

$$\mathcal{L}_G = \frac{1}{16\pi G}R, \tag{2}$$

*Electronic address: sugar@dec.rikadai.jp
†Electronic address: sawado@ph.noda.tus.ac.jp
‡Electronic address: norikoshiiki@mail.goo.ne.jp

$$\mathcal{L}_S = \frac{f_\pi^2}{16} g^{\mu\nu} \mathrm{Tr}(U^{-1}\partial_\mu U U^{-1}\partial_\nu U) + \frac{1}{32e^2} g^{\mu\rho} g^{\nu\sigma} \mathrm{Tr}([U^{-1}\partial_\mu U, U^{-1}\partial_\nu U] \times [U^{-1}\partial_\rho U, U^{-1}\partial_\sigma U]), \quad (3)$$

where f_π is pion decay constant and e is a dimensionless free parameter. U describes the $SU(2)$ chiral fields. We impose the axially symmetric ansatz on the chiral fields as a possible candidate for the $B = 2$ minimal energy configuration [6]

$$U = \cos F(r, \theta) + i\boldsymbol{\tau} \cdot \boldsymbol{n}_R \sin F(r, \theta), \quad (4)$$

with

$$\boldsymbol{n}_R = (\sin\Theta(r, \theta) \cos n\varphi, \sin\Theta(r, \theta) \sin n\varphi, \cos\Theta(r, \theta)), \quad (5)$$

where n denotes the winding number of solitons, which is equivalent to the baryon number B. Since we are interested in $B = 2$ skyrmions, we consider only $n = 2$. Correspondingly, the following axially symmetric ansatz is imposed on the metric [11]

$$ds^2 = -f dt^2 + \frac{m}{f}(dr^2 + r^2 d\theta^2) + \frac{l}{f} r^2 \sin^2\theta d\varphi^2, \quad (6)$$

where the metric functions f, m,and l are the function of

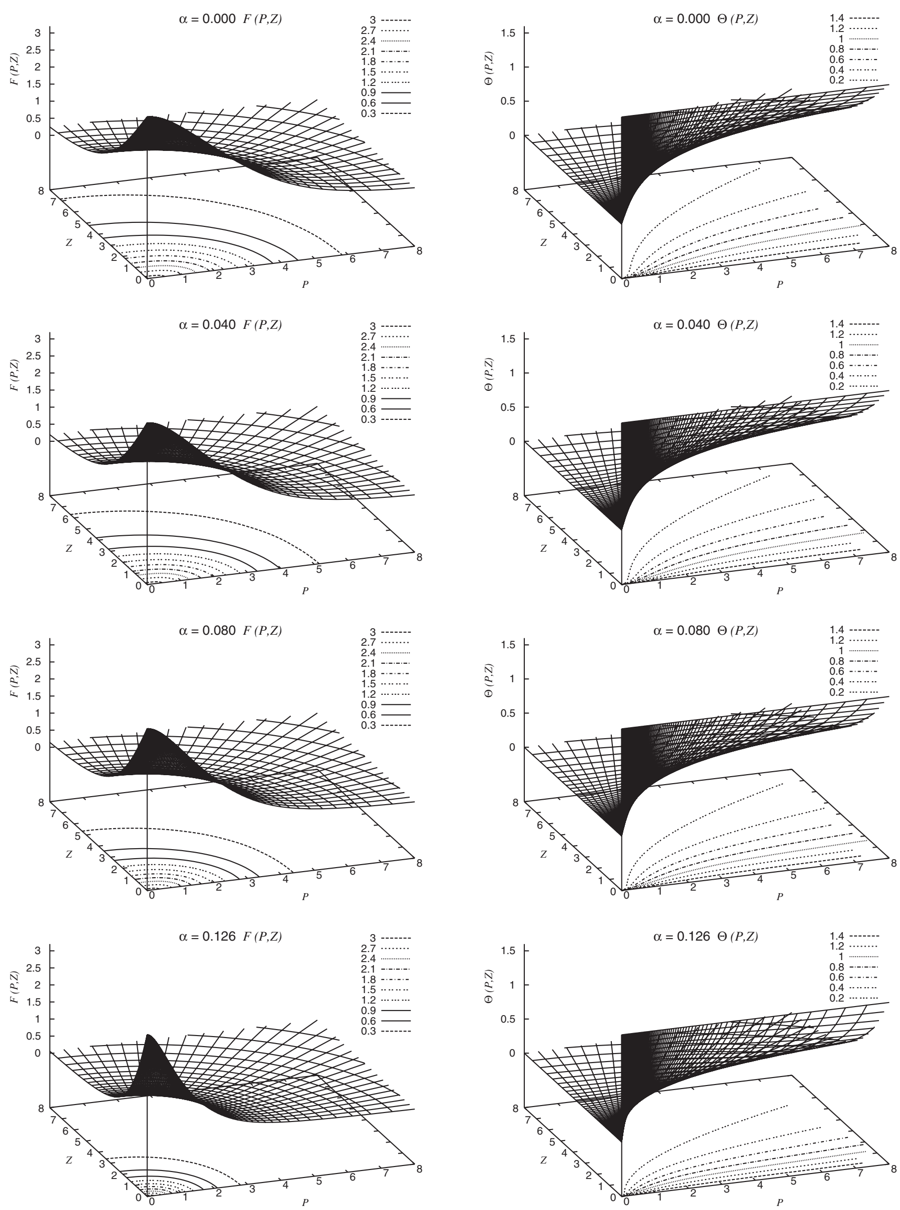

FIG. 1. The profile function F and Θ in the cylindrical coordinate with $\alpha = 0.000$, 0.040, 0.080, 0.126 are shown. We use dimensionless variables $P = ef_\pi\rho$ and $Z = ef_\pi z$. There exists no solution for $\alpha \gtrsim 0.127$.

coordinates r and θ. This metric is symmetric with respect to the z xis ($\theta = 0$). Substituting these ansatz to the Lagrangian (3), one obtains the following static energy density for the chiral fields

$$\begin{aligned}\varepsilon(x, \theta) = \frac{\sqrt{l}\sin\theta}{8}\Big\{&x^2((\partial_x F)^2 + (\partial_x \Theta)^2 \sin^2 F) + (\partial_\theta F)^2 \\ &+ (\partial_\theta \Theta)^2 \sin^2 F + \frac{n^2 m}{l \sin\theta}\sin^2 F \sin^2 \Theta\Big\} \\ &+ \frac{\sqrt{l}\sin\theta}{2}\Big[\frac{f}{m}(\partial_x F \partial_\theta \Theta - \partial_\theta F \partial_x \Theta)^2 \sin^2 F \\ &+ \frac{n^2 f}{l \sin^2\theta}\sin^2 F \sin^2 \Theta \Big\{\Big((\partial_x F)^2 + \frac{1}{x^2}(\partial_\theta F)^2\Big) \\ &+ \Big((\partial_x \Theta)^2 + \frac{1}{x^2}(\partial_\theta \Theta)^2\Big)\sin^2 F\Big\}\Big], \end{aligned} \tag{7}$$

where dimensionless variable $x = ef_\pi r$ is introduced. The static (classical) energy is thus given by

$$M = 2\pi \frac{f_\pi}{e} \int dx d\theta \varepsilon(x, \theta). \tag{8}$$

The covariant topological current is defined by

$$B^\mu = \frac{\epsilon^{\mu\nu\rho\sigma}}{24\pi^2} \frac{1}{\sqrt{-g}} \operatorname{tr}(U^{-1}\nabla_\nu U U^{-1} \nabla_\rho U U U^{-1} \nabla_\sigma U), \tag{9}$$

whose zeroth component corresponds to the baryon number density

$$B^0 = -\frac{1}{\pi^2 \sqrt{-g}} \sin^2 F \sin\Theta(\partial_x F \partial_\theta \Theta - \partial_\theta F \partial_x \Theta). \tag{10}$$

For the solutions to be regular at the origin $x = 0$ and to be asymptotically flat at infinity, the following boundary conditions must be imposed:

$$\partial_x f(0, \theta) = \partial_x m(0, \theta) = \partial_x l(0, \theta) = 0, \tag{11}$$

$$f(\infty, \theta) = m(\infty, \theta) = l(\infty, \theta) = 1. \tag{12}$$

For the configuration to be axially symmetric, the following boundary conditions must be imposed at $\theta = 0$ and $\pi/2$:

$$\partial_\theta f(x, 0) = \partial_\theta m(x, 0) = \partial_\theta l(x, 0) = 0, \tag{13}$$

$$\partial_\theta f\Big(x, \frac{\pi}{2}\Big) = \partial_\theta m\Big(x, \frac{\pi}{2}\Big) = \partial_\theta l\Big(x, \frac{\pi}{2}\Big) = 0. \tag{14}$$

For the profile functions, the boundary conditions at the $x = 0, \infty$ are given by

$$F(0, \theta) = \pi, \qquad F(\infty, \theta) = 0, \tag{15}$$

$$\partial_x \Theta(0, \theta) = \partial_x \Theta(\infty, \theta) = 0. \tag{16}$$

At $\theta = 0$ and $\pi/2$,

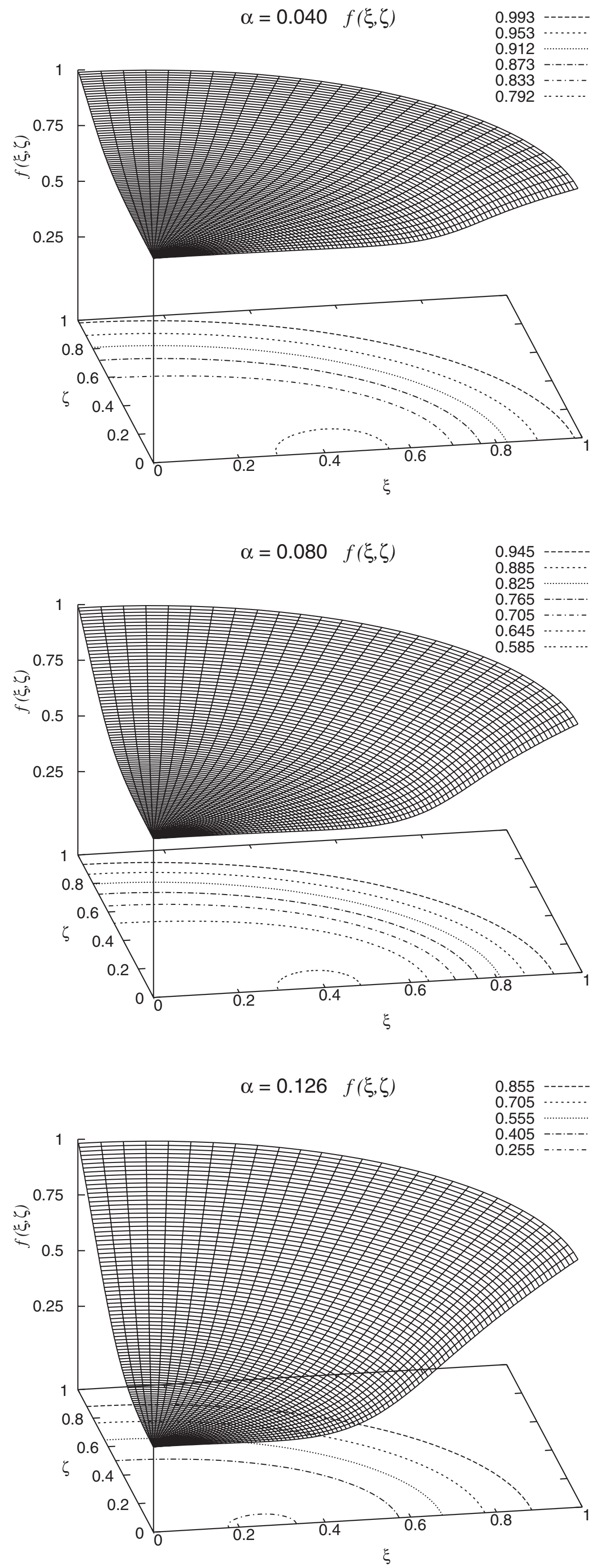

FIG. 2. The metric function f in the cylindrical coordinate with $\alpha = 0.040$, 0.080, 0.126 is shown. We use $\xi = P/(1 + P)$ and $\zeta = Z/(1 + Z)$, instead of dimensionless variables $P = ef_\pi \rho$ and $Z = ef_\pi z$.

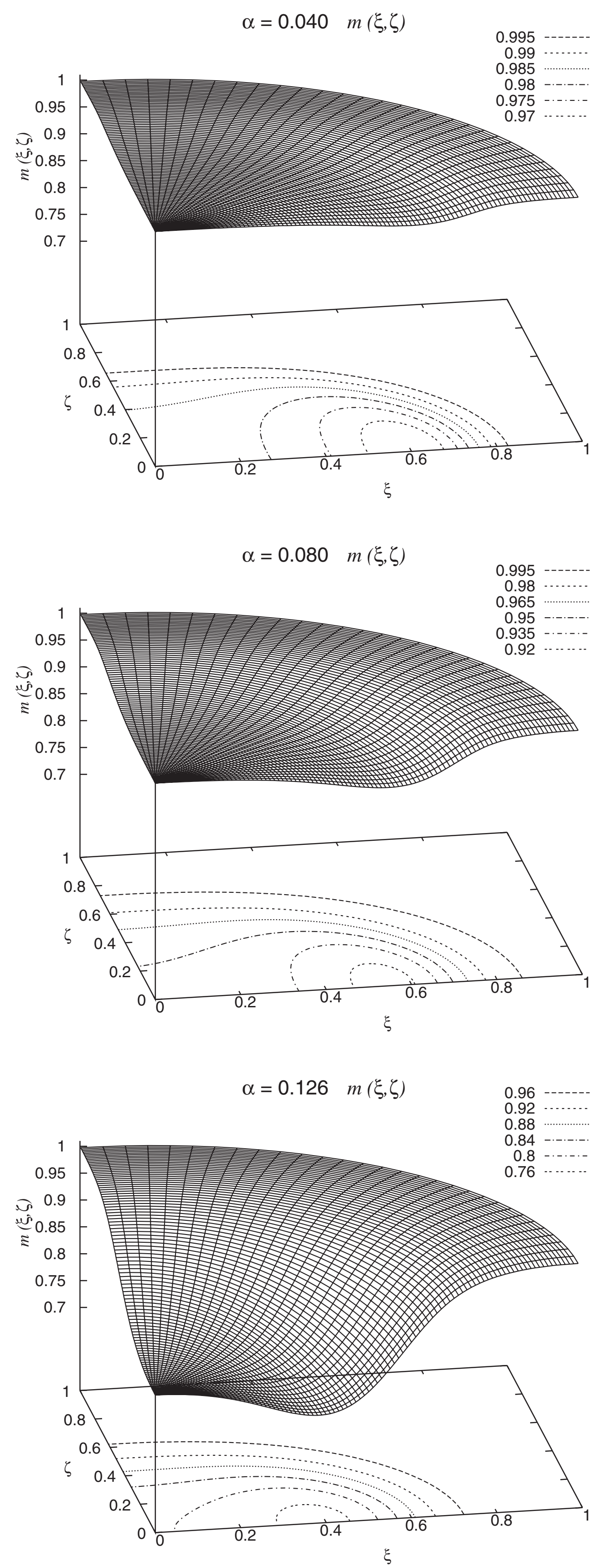

FIG. 3. Same as Fig. 2 for the metric function m.

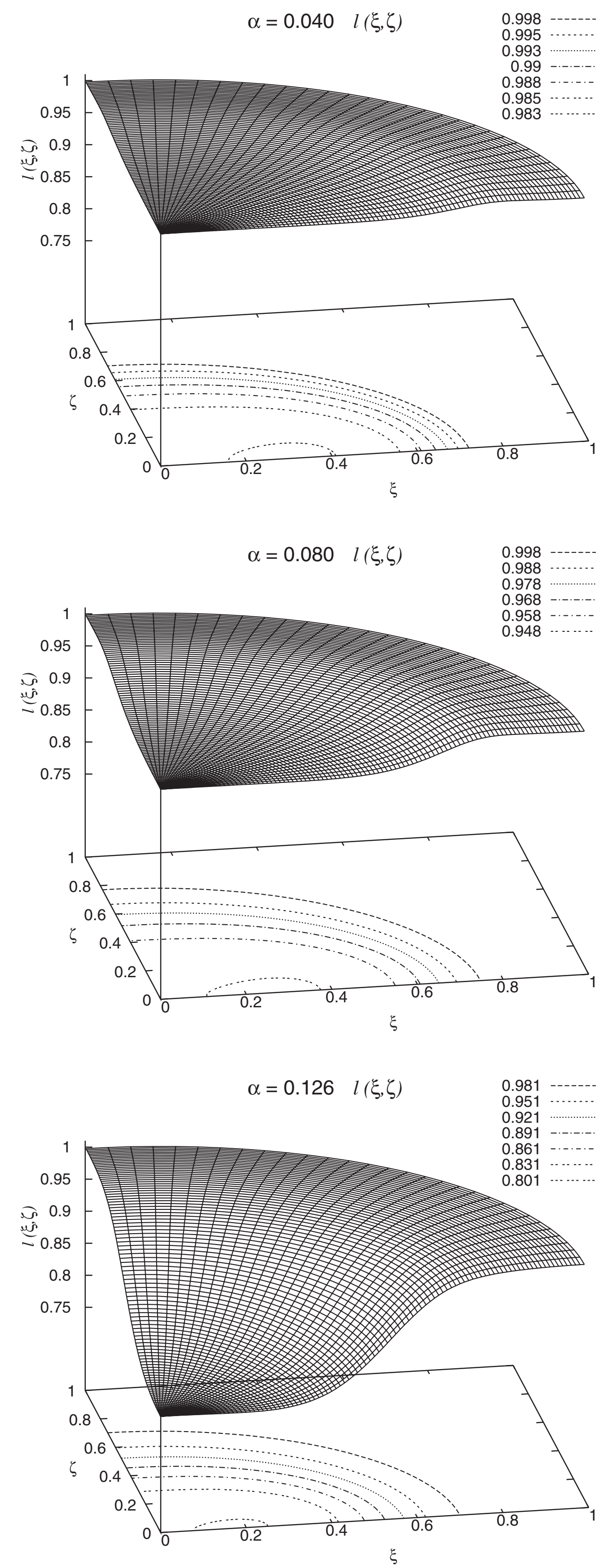

FIG. 4. Same as Fig. 2 for the metric function l.

$$\partial_\theta F(x, 0) = \partial_\theta F\left(x, \frac{\pi}{2}\right) = 0, \tag{17}$$

$$\Theta(x, 0) = 0, \qquad \Theta\left(x, \frac{\pi}{2}\right) = \frac{\pi}{2}. \tag{18}$$

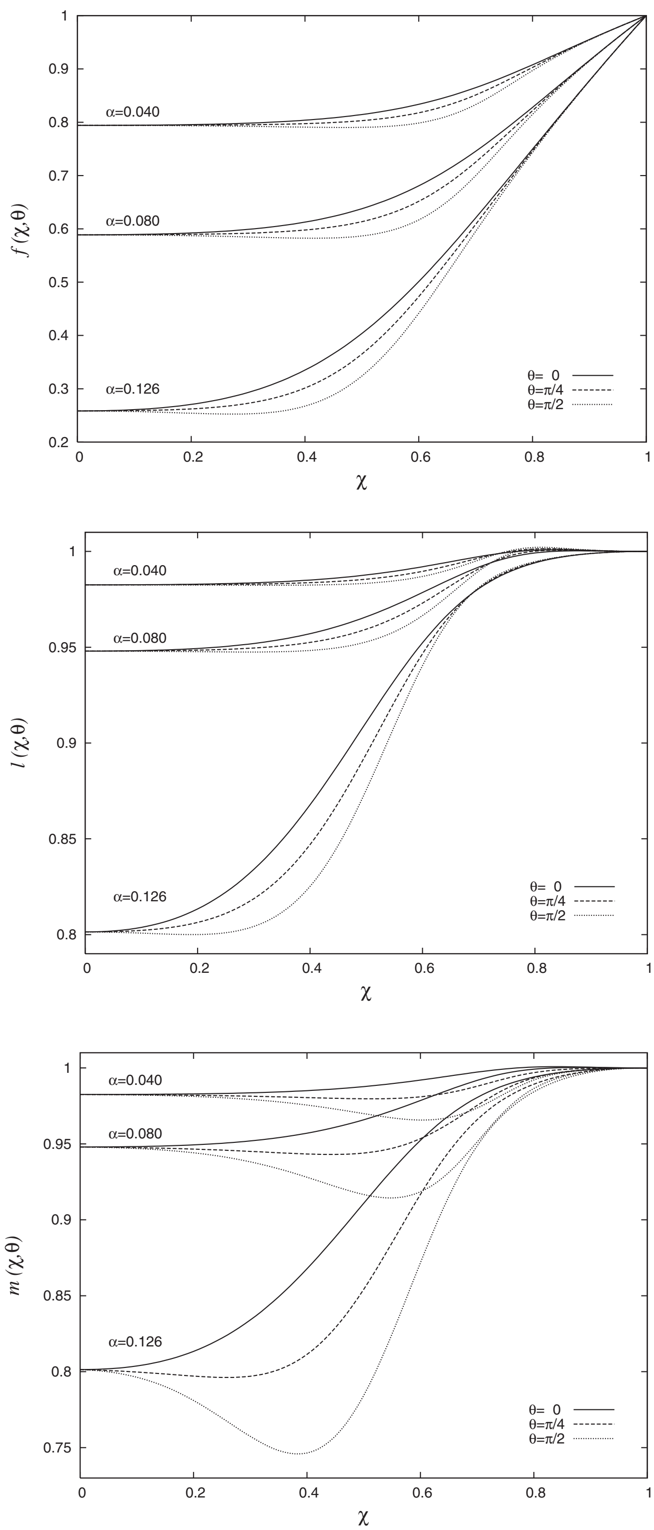

FIG. 5. The metric function f, m and l for $\theta = 0$, $\pi/4$, $\pi/2$ as a function of radial coordinate with $\alpha = 0.040, 0.080, 0.126$ are shown. We use $\chi = x/(1 + x)$, instead of dimensionless variable $x = ef_\pi r$.

Since the baryon number is defined by the spatial integral of the zeroth component of the baryon current, we have

$$B = \int d^3r\sqrt{-g}B^0 = \frac{1}{2\pi}(2F - \sin 2F)\cos\Theta \Big|_{F_0,\Theta_0}^{F_1,\Theta_1}. \tag{19}$$

The inner and outer boundary conditions $(F_0, \Theta_0) = (\pi, 0)$ and $(F_1, \Theta_1) = (0, \pi)$ yield $B = 2$.

By taking a variation of the static energy (7) with respect to F and Θ, one obtains the equations of motion for the profile functions. The field equations for the metric functions f, m, and l are derived from the Einstein equations. We shall show their explicit form in the appendix.

The effective coupling constant of the Einstein-Skyrme system is given by

$$\alpha = 4\pi G f_\pi^2, \tag{20}$$

which is the only free parameter.

We use the relaxation method to solve these nonlinear equations with the typical grid size 100×30. In Fig. 1, the profile functions for $\alpha = 0, 0.04, 0.08, 0.126$ is presented. No solution exists for $\alpha \gtrsim 0.127$. Also, the metric functions are shown in Figs. 2–4. In Fig. 5, we display the metric functions at $\theta = 0$, $\pi/4$, $\pi/2$ as a function of radial coordinate. Figure 6 shows α dependence of the static energy M in unit of f_π/e. In Fig. 7 the energy densities defined in Eq. (7) are plotted. The baryon densities $b = \sqrt{-g}B^0$ are shown in Fig. 8.

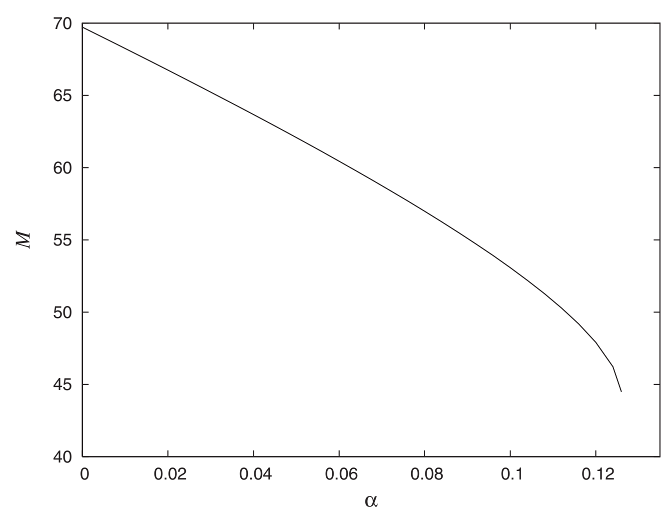

FIG. 6. The coupling constant dependence of the classical $B = 2$ skyrmion dimensionless mass derived from Eq. (8).

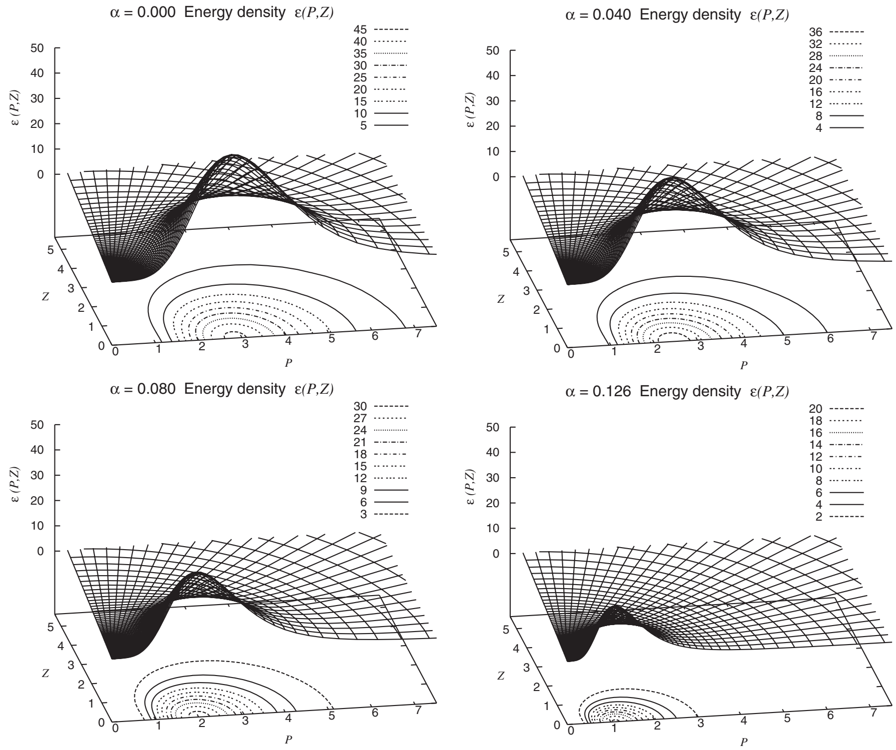

FIG. 7. The energy density ε in the cylindrical coordinate with $\alpha = 0.000$, 0.040, 0.080, 0.126 are shown, in terms of the dimensionless variables $P = ef_\pi\rho$ and $Z = ef_\pi z$.

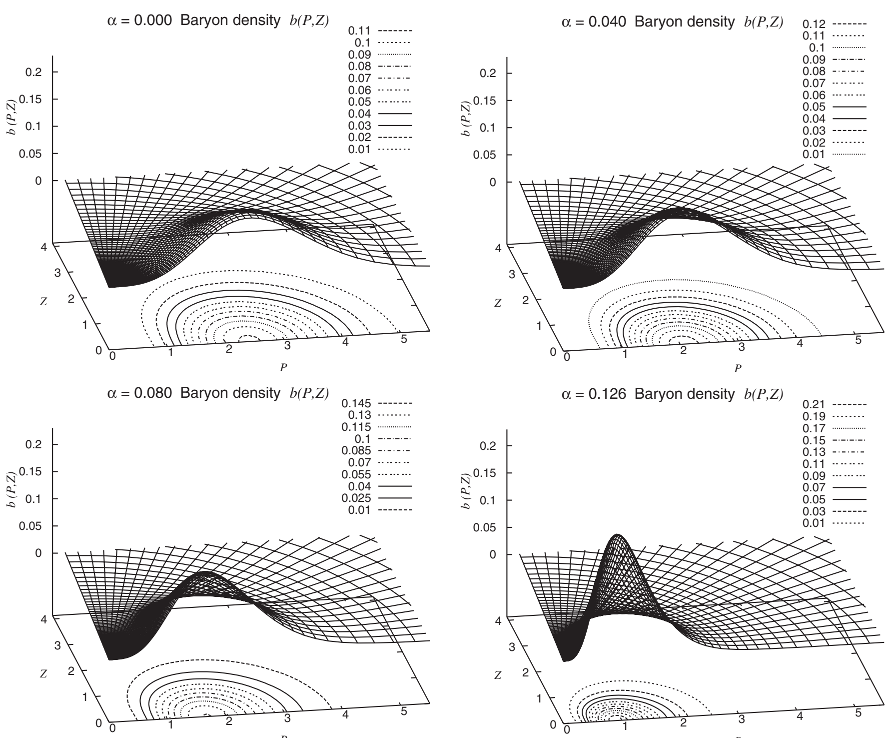

FIG. 8. The baryon density $b = \sqrt{-g}B^0$ in the cylindrical coordinate with $\alpha = 0.000$, 0.040, 0.080, 0.126 are shown, in terms of the dimensionless variables $P = ef_\pi\rho$ and $Z = ef_\pi z$.

III. COLLECTIVE QUANTIZATION SCHEME FOR THE $B = 2$ SOLITON SOLUTION

In this section, let us try to give an interpretation to the $B = 2$ skyrmion solution obtained in the last section as a baryonic object by assigning quantum number of spin and isospin to it. We employ the semiclassical zero-mode quantization following Ref. [6]. Let us introduce dynamically rotated chiral fields

$$\hat{U}(\boldsymbol{r}, t) = A(t)U(\boldsymbol{r}')A^\dagger(t), \qquad \boldsymbol{r}' = R(B(t))\boldsymbol{r}, \tag{21}$$

and

$$R_{ij}(B) = \tfrac{1}{2}\mathrm{Tr}(\boldsymbol{\tau}_i B \boldsymbol{\tau}_j B^\dagger), \tag{22}$$

where $A(t)$ and $B(t)$ are the time-dependent $SU(2)$ matrices generating the isospin and the spatial rotations. Substituting (21) into the Lagrangian (3), one finds

$$L = -M + \tfrac{1}{2}a_i U_{ij} a_j - a_i W_{ij} b_j + \tfrac{1}{2} b_i V_{ij} b_j, \tag{23}$$

where M is the static energy of the $B = 2$ skyrmion given in Eq. (8). The Lagrangian is quadratic in time derivatives

$$a_i = -i\,\mathrm{Tr}\tau_i A^\dagger \dot{A}, \qquad b_i = i\,\mathrm{Tr}\tau_i \dot{B} B^\dagger. \tag{24}$$

The moments of inertia tensor U_{ij}, V_{ij}, and W_{ij} are expressed in terms of the chiral field U as

$$U_{ij} = \frac{1}{8f_\pi e^3}\int d^3x \bigg[\frac{m\sqrt{l}}{f^2}x^2 \sin\theta \bigg\{\mathrm{Tr}\bigg(U^\dagger\bigg[\frac{\boldsymbol{\tau}_i}{2}, U\bigg]U^\dagger\bigg[\frac{\boldsymbol{\tau}_j}{2}, U\bigg]\bigg) + g^{kl}\mathrm{Tr}\bigg[U^\dagger\partial_k U, U^\dagger\bigg[\frac{\boldsymbol{\tau}_i}{2}, U\bigg]\bigg] \times \bigg[U^\dagger\partial_l U, U^\dagger\bigg[\frac{\boldsymbol{\tau}_j}{2}, U\bigg]\bigg]\bigg\}\bigg], \tag{25}$$

$$W_{ij} = U_{ij}\bigg\{\bigg[\frac{\boldsymbol{\tau}_j}{2}, U\bigg] \to i(\boldsymbol{x}' \times \nabla)_j U)\bigg\}, \tag{26}$$

$$V_{ij} = W_{ij}\bigg\{\bigg[\frac{\boldsymbol{\tau}_i}{2}, U\bigg] \to i(\boldsymbol{x}' \times \nabla)_i U)\bigg\}. \tag{27}$$

Body-fixed isospin operator K_i and angular momentum operator L_i are defined as a canonically conjugate to a_i and b_i

$$K_i = \frac{\partial L}{\partial a_i} = U_{ij}a_j - W_{ij}b_j, \qquad L_i = \frac{\partial L}{\partial b_i} = -W_{ij}^T a_j + V_{ij}b_j. \tag{28}$$

These operators are related to the usual coordinate-fixed isospin I_i and spin J_i by the orthogonal transformation,

$$I_i = -R_{ij}(A)K_j, \qquad J_i = -R_{ij}(B)^T L_j. \tag{29}$$

The commutation relations for these operators are

$$[K_i, K_j] = i\epsilon_{ijk}K_k, \qquad [L_i, L_j] = i\epsilon_{ijk}L_k, \qquad [I_i, I_j] = i\epsilon_{ijk}I_k, \qquad [J_i, J_j] = i\epsilon_{ijk}J_k. \tag{30}$$

These operators satisfy the Casimir invariance by using Eq. (29)

$$\boldsymbol{K}^2 = \boldsymbol{I}^2, \qquad \boldsymbol{L}^2 = \boldsymbol{J}^2. \tag{31}$$

The symmetry of the classical soliton induces the following conditions for the inertia tensors

$$U_{11} = U_{22}, \quad V_{11} = V_{22}, \quad W_{11} = W_{22} = 0, \quad V_{33} = 4U_{33}, \quad W_{33} = 2U_{33}. \tag{32}$$

Thus it is sufficient to calculate only U_{11}, U_{33}, and V_{11}. Inserting (4) into Eqs. (25) and (27) one obtains

$$U_{11} = \frac{\pi}{f_\pi e^3}\int dx d\theta \bigg[\frac{m\sqrt{l}}{4f^2}x^2 \sin\theta \sin^2 F(1 + \cos^2\Theta) + \frac{\sqrt{l}}{f}\sin\theta\sin^2 F\bigg\{(1 + \cos^2\Theta)(x^2 F_{,x}^2 + F_{,\theta}^2) + \sin^2 F\cos^2\Theta(x^2\Theta_{,x}^2 + \Theta_{,\theta}^2) + \frac{n^2 m}{l\sin^2\theta}\sin^2 F\sin^2\Theta\bigg\}\bigg], \tag{33}$$

$$U_{33} = \frac{\pi}{f_\pi e^3}\int dx d\theta \bigg[\frac{m\sqrt{l}}{2f^2}x^2 \sin\theta\sin^2 F\sin^2\Theta + \frac{2\sqrt{l}}{f}\sin\theta\sin^2 F\sin^2\Theta\bigg\{x^2 F_{,x}^2 + F_{,\theta}^2 + \sin^2 F(x^2\Theta_{,x}^2 + \Theta_{,\theta}^2)\bigg\}\bigg], \tag{34}$$

$$V_{11} = \frac{\pi}{f_\pi e^3}\int dx d\theta \bigg[\frac{m\sqrt{l}}{4f^2}x^2 \sin\theta(F_{,x}^2 + \Theta_{,\theta}^2\sin^2 F + n^2\cot^2\theta\sin^2 F\sin^2\Theta) + \frac{\sqrt{l}}{f}x^2\sin\theta\sin^2 F\{(F_{,x}\Theta_{,\theta} - F_{,\theta}\Theta_{,x})^2 + n^2(F_{,x}^2 + \Theta_{,x}^2\sin^2 F)\cot^2\theta\sin^2\Theta\} + \frac{n^2\sqrt{l}}{f\sin\theta}\bigg(\cos^2\theta + \frac{m}{l}\bigg)(F_{,\theta}^2 + \Theta_{,\theta}^2\sin^2 F)\sin^2 F\sin^2\Theta\bigg]. \tag{35}$$

From Eqs. (28) and (32) we derive the constraint

$$(2K_3 + L_3)|\mathrm{phys}\rangle = 0. \tag{36}$$

Inserting the body-fixed operator (28), Casimir invariant (31), and constraint (36) into the Lagrangian (23) one can get the Hamiltonian operator as

$$H = M + \frac{\boldsymbol{I}^2}{2U_{11}} + \frac{\boldsymbol{J}^2}{2V_{11}} + \bigg[\frac{1}{U_{33}} - \frac{1}{U_{11}} - \frac{4}{V_{11}}\bigg]\frac{K_3^2}{2}. \tag{37}$$

TABLE I. The dimensionless quantized energy spectra up to $i, j \leq 3$ for $\kappa = 0$, and also some excited states up to $\kappa \leq 2$. In the particle classification, we give the baryonic descriptions if available, otherwise we only show its spectroscopic classification $^{2s+1}L_j$.

Classification	i	j	κ	Parity	$\alpha = 0$	$\alpha = 0.040$	$\alpha = 0.080$	$\alpha = 0.126$
Classical skyrmion					69.7195	63.6722	56.9827	44.4862
Deuteron ($^3S_1$)	0	1	0	+	69.7227	63.6758	56.9866	44.4912
NN ($^1S_0$)	1	0	0	+	69.7241	63.6774	56.9886	44.4939
($^3P_2$)	1	2	1	−	69.7294	63.6828	56.9943	44.5006
NΔ ($^5S_2$)	1	2	0	+	69.7339	63.6881	57.0003	44.5089
NΔ ($^3S_2$)	2	1	0	+	69.7368	63.6913	57.0041	44.5143
($^3P_2$)	2	2	1	−	69.7387	63.6932	57.0059	44.5160
ΔΔ ($^7S_3$)	0	3	0	+	69.7391	63.6935	57.0062	44.5162
($^5P_3$)	1	3	1	−	69.7392	63.6935	57.0060	44.5156
ΔΔ ($^1S_0$)	3	0	0	+	69.7475	63.7032	57.0176	44.5324
($^5D_4$)	2	4	2	+	69.7479	63.7024	57.0153	44.5262
($^5P_3$)	2	3	1	−	69.7485	63.7039	57.0177	44.5310

The corresponding energy (mass) eigenvalues are

$$E = M + \frac{i(i+1)}{2U_{11}} + \frac{j(j+1)}{2V_{11}} + \left[\frac{1}{U_{33}} - \frac{1}{U_{11}} - \frac{4}{V_{11}}\right]\frac{\kappa^2}{2}, \tag{38}$$

where $i(i+1)$, $j(j+1)$, and κ are the eigenvalues of the Casimir operators (31), and the operator K_3, respectively. The parity is defined by the eigenstate of the following operator:

$$P = e^{i\pi K_3}, \tag{39}$$

which means that the parity is (+) for even κ and (−) for odd κ.

Taking into account the Finkelstein-Rubinstein constraints for the axially symmetric soliton [6], one finds that some combinations of (i, j) are not acceptable. The allowed states are [6,12]

$$|ii_3 0\rangle|jj_3 0\rangle, \ \text{provided } i+j \text{ is odd}, \qquad (\text{for } \kappa = 0)$$
$$\frac{1}{\sqrt{2}}[|ii_3\kappa\rangle|jj_3 - 2\kappa\rangle - (-1)^{i+j}|ii_3 - \kappa\rangle|jj_3 2\kappa\rangle]$$
$$(\text{for } \kappa = 1, \cdots, \min\{i, [j/2]\}). \tag{40}$$

Therefore, $\kappa > 0$ is allowed only if $i \geq 1$ and $j \geq 2$.

We show quantized energy spectra for various values of α in Table I. The mass difference from the classical energy is shown as a function of α in Fig. 9. In Table I (and Fig. 9), we show the results for $i, j \leq 3$ with $\kappa = 0$, and also some excited states for $\kappa \leq 2$. We present a spectroscopic classification $^{2s+1}L_j$ in Table I. For $\kappa = 0$, the system is in S state, and then j equals to the intrinsic spin s. For $\kappa > 0$ state, the orbital angular momentum is chosen to be its lowest value so that it is consistent with the quantum number j, the parity, and the fact that $s \leq 3$ in the six-quark picture. It is seen that the mass difference increases monotonically with increasing α. Figure 1 (and also Figs. 7

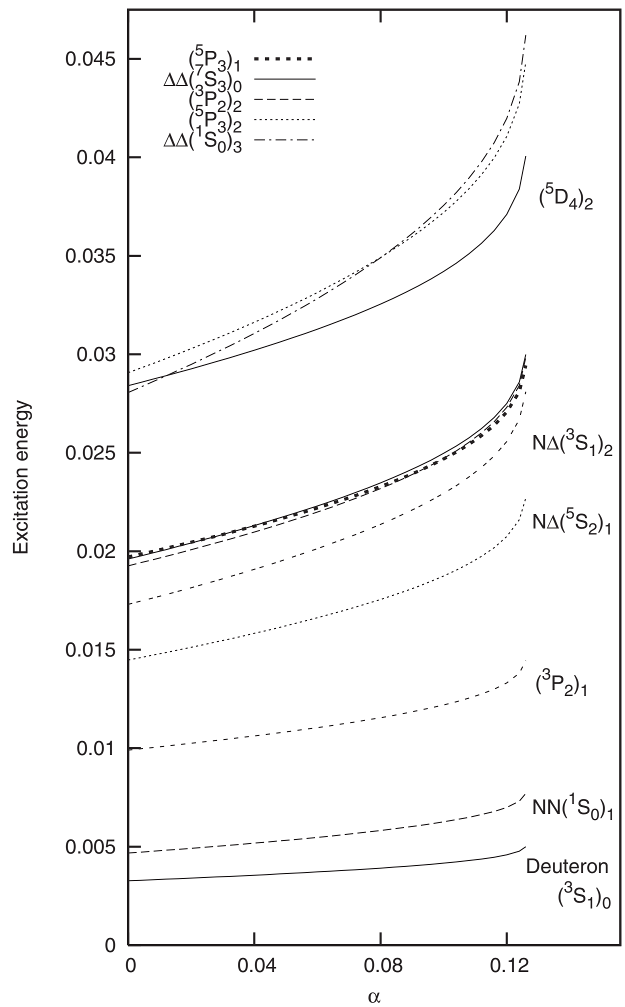

FIG. 9. The coupling constant dependence of the dimensionless mass difference from the classical energy are shown. For $\alpha \gtrsim 0.127$, there exists no solution. We give the baryonic descriptions if available, otherwise we only show its spectroscopic classification $(^{2s+1}L_j)_i$, whose subscript i means eigenvalue of the isospin operator (31).

and 8) implies that the strong gravity makes the size of the skyrmion smaller which makes the inertial moment smaller, resulting in increase in the mass difference. In the collective quantization, the skyrmion can be quantized as a slowly rotating rigid body and the mass difference is interpreted as a consequence of the rotational kinetic energy. Thus the gravity works for increasing the kinetic energy of the skyrmion. In the naïve quark model picture, the mass difference is ascribed to the hyperfine splittings. The increase in the mass difference may imply that due to the reduction of the distance between quarks, the effects of the hyperfine splittings become dominant by the gravity [13].

From the data of Table I, one can straightforwardly obtain the mass value in MeV unit by multiplying f_π/e for any parameter choice (f_π, e). With $f_\pi = 108$ MeV, $e = 4.84$, which is used in Ref. [6], our obtained mass value in the case of $\alpha = 0$ is approximately 6% lower than the value obtained in Ref. [6]. There are two possible reasons for that. First, the Lagrangian in Ref. [6] includes the mass term and hence it slightly enhances the mass value. Thus we also performed the same analysis including the mass term, which reduced the error from 6% to 0.5% in the mass. Second, the coordinate system they used is cylindrical while we adopted the spherical coordinates. Since the cylindrical coordinate requires a much larger number of grid points to obtain torus-shape solutions than the spherical, we suspect that their results are not fully convergent, producing a slightly larger mass.

IV. ELECTROMAGNETIC PROPERTIES

In this section we shall investigate the gravity effects to the various observables, i.e. the mean charge radius $\langle r^2\rangle_d^{1/2}$, magnetic moment μ_d, the quadrupole moment Q, and the transition moment $\mu_{d\to np}$, which is associated with the process $\gamma d \to {}^1S_0$.

Let us introduce the electromagnetic current in the Skyrme model $J_\mu^{(\mathrm{em})}(x)$ which consists of the isoscalar and isovector part,

$$J_\mu^{(\mathrm{em})}(x) = \frac{1}{2}B_\mu(x) + I_\mu^3(x), \tag{41}$$

where $B_\mu(x)$ is baryon current density given in Eq. (9) and $I_\mu^3(x)$ is the third component of the isospin current density, defined by

$$I_\mu^a(x) = -ef_\pi^3\frac{i}{8}\bigg(g^{\mu\nu}\,\mathrm{Tr}\bigg[U^{-1}\bigg[\frac{\boldsymbol{\tau}_i}{2}, U\bigg]U^{-1}\partial_\mu U\bigg] + g^{\mu\rho}g^{\nu\sigma}\,\mathrm{Tr}\bigg[U^{-1}\bigg[\frac{\boldsymbol{\tau}_i}{2}, U\bigg]U^{-1}\partial_\nu U\bigg] \times [U^{-1}\partial_\mu U, U^{-1}\partial_\nu U]\bigg). \tag{42}$$

Inserting the dynamical field $\hat{U}$ in Eq. (21) into Eq. (41) gives electromagnetic current operator $\hat{J}_\mu^{(\mathrm{em})}$.

To estimate the expectation value of these quantum operators, we describe the quantum spin states (40) in terms of the products of the rotation matrices

$$\langle A|ii_3k_3\rangle = \bigg(\frac{2i+1}{8\pi^2}\bigg)^{1/2}D^i(i\tau^2A^\dagger)_{k_3i_3}, \tag{43}$$

$$\langle B|jj_3l_3\rangle = \bigg(\frac{2j+1}{8\pi^2}\bigg)^{1/2}D^j(i\tau^2B^\dagger)_{j_3l_3}. \tag{44}$$

where $D^i(A)_{m,m'}$ is the well-known Wigner D function. The computation can be performed easily by the following integration formula [14]:

$$\int dBD^i(B)^*_{m_1m_1'}D^j(B)_{m_2m_2'}D^k(B)_{m_3m_3'} = \frac{8\pi^2}{2k+1}C^{km_3}_{im_1jm_2}C^{km_3'}_{im_1'jm_2'}, \tag{45}$$

where $C^{km_3}_{im_1jm_2}$ is a Clebsch-Gordan coefficient.

The deuteron charge radius $\langle r^2\rangle_d^{1/2}$ is defined as the square root of

$$\langle r^2\rangle_d \equiv \bigg\langle d\bigg|\int d^3r r^2\hat{J}_0^{(\mathrm{em})}(\boldsymbol{r}, t)\bigg|d\bigg\rangle, \tag{46}$$

where $|d\rangle$ represents spin state of the deuteron. In this case, as only the isoscalar part of $\hat{J}_0^{(\mathrm{em})}$ contributes to the matrix element, the integration is straightforward:

$$\begin{aligned}\langle r^2\rangle_d &= \frac{\pi}{(ef_\pi)^2}\int dxd\theta\sqrt{-g}x^2B^0(r,\theta)\\ &= -\frac{1}{\pi(ef_\pi)^2}\int dxd\theta x^2\sin^2F\sin\Theta(\partial_xF\partial_\theta\Theta\\ &\quad - \partial_\theta F\partial_x\Theta).\end{aligned} \tag{47}$$

Figure 10 shows the α dependence of the mean charge radius. Because of the attractive effect of the gravity, it decreases with increasing α.

The isoscalar part of the magnetic moments is expressed in terms of an electromagnetic current as

$$\hat{\mu}_i = \frac{1}{2}\int d^3r\sqrt{-g}\epsilon_{ijk}r_j\hat{J}_0^{(\mathrm{em})}(\boldsymbol{r}, t). \tag{48}$$

Inserting the dynamical field $\hat{U}$ in Eq. (21) into Eq. (48), one finds the magnetic momentum operator as

$$\hat{\mu}_i|_{I=0} = \frac{1}{2}\{R_{ij}(B)^T, \mu_{jk}a_k + \mu'_{jk}b_k\}, \tag{49}$$

where

$$\mu_{jk} = \frac{1}{(ef_\pi)^2}\int d^3x\frac{1}{2}\varepsilon_{jlm}x_l\frac{1}{2}\,\mathrm{Tr}\bigg[U^\dagger\bigg[\frac{1}{2}\boldsymbol{\tau}_k, U\bigg]C_m\bigg], \tag{50}$$

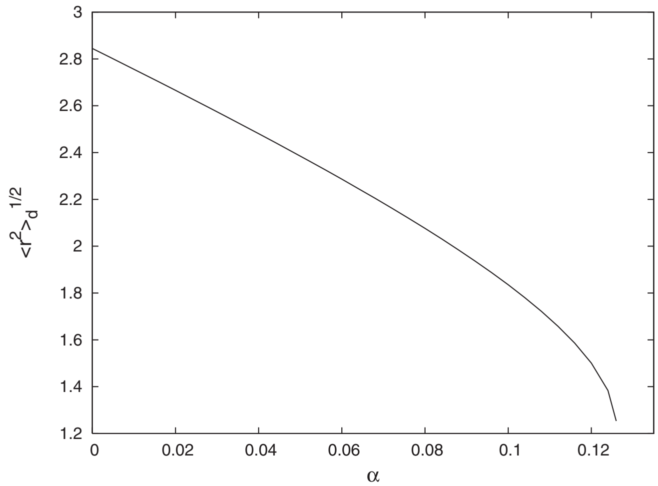

FIG. 10. The coupling constant dependence of the dimensionless mean charge radius (47).

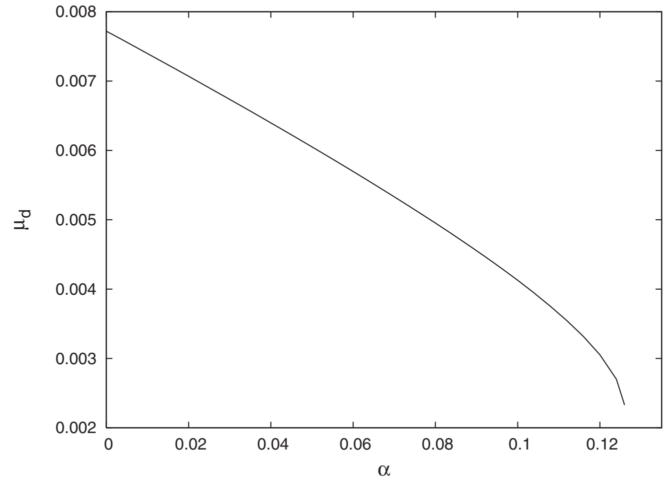

FIG. 11. The coupling constant dependence of the dimensionless magnetic moment (55).

$$\mu'_{jk} = \frac{1}{(ef_\pi)^2} \int d^3x \frac{1}{2} \varepsilon_{jlm} x_l \frac{1}{2} \mathrm{Tr}[U^\dagger(-i\boldsymbol{x} \times \boldsymbol{\nabla})_k U C_m(\boldsymbol{x})], \tag{51}$$

and C_m is

$$C_m(\boldsymbol{x}) = \frac{i}{8\pi^2} \varepsilon_{mnp} (U^\dagger \partial_n U)(U^\dagger \partial_p U). \tag{52}$$

The R_{ij} is the rotation matrix (22) and a_i and b_i are defined as Eq. (24). The anticommutator relation in Eq. (48) guarantees $\hat{\mu}_i$ to be a Hermitian operator. μ_{ij} and μ'_{jk} are diagonal and furthermore they satisfy $\mu_{11} = \mu_{22} = 0$, $\mu'_{11} = \mu'_{22}$, and $\mu'_{33} = -2\mu_{33}$. With these relations and using the body-fixed operator (28), the coordinate-fixed operator (29), the relation of the moment of inertia components (32), and the constraint of Eq. (36) in Eq. (48), one can get

$$\hat{\mu}_i|_{I=0} = -\frac{\mu'_{11}}{V_{11}} \boldsymbol{J}_l + \text{ terms proportional to } K_3. \tag{53}$$

Therefore, we only use the component of μ'_{11},

$$\mu'_{11} = -\frac{\pi}{4(ef_\pi)^2} \int dx d\theta \sqrt{-g} x^2 (\cos^2\theta + 1) B_0(x, \theta). \tag{54}$$

And the V_{11} is the moment of inertia given in Eq. (35). The moments μ_d of deuteron is defined as the expectation value of the $\hat{\mu}_3$ with $j_3 = 1$

$$\mu_d = \langle \hat{\mu}_3 \rangle = -\frac{\mu'_{11}}{V_{11}}. \tag{55}$$

In Fig. 11 α dependence of the μ_d is shown. It decreases with increasing α, but the effect of gravity is more evident compared with that of $B = 1$ [10]. In the nonrelativistic nuclear physics point of view, the magnetic moment of the deuteron consists of the sum of the magnetic moment of the proton plus neutron and some correction terms related to the D-state probability of the deuteron. This result indicates that the assumption that the deuteron is almost S state (contributions to the other states are only $\sim$5%) may no longer be valid under the strong gravitational field. Therefore, we speculate that the effect of gravity is apparent on the change of such noncentral components of the nuclear force. This will be more evident by examining the quadrupole moment. The quadrupole moment is given by

$$\hat{Q}_{ij} = \int d^3r \sqrt{-g} (3r_i r_j - r^2 \delta_{ij}) \hat{J}_0^{(\mathrm{em})}(\boldsymbol{r}, \theta), \tag{56}$$

which is the same as the magnetic moment. Inserting (21) into Eq. (56) one obtains the quadrupole momentum operator

$$\hat{Q}_{ij}|_{I=0} = R_{ia}(B)^T Q_{ab} R_{bj}(B), \tag{57}$$

where

$$Q_{ab} = \frac{1}{2(ef_\pi)^2} \int d^3x \sqrt{-g} (3x_a x_b - x^2 \delta_{ab}) B_0(x, \theta). \tag{58}$$

Q_{ij} satisfies $Q_{11} = Q_{22}$. And the symmetry relation for the quadrupole moments reduces the expression to

$$\hat{Q}_{ij}|_{I=0} = Q_{33}[\tfrac{3}{2} R_{i3}(B)^T R_{3j}(B) - \tfrac{1}{2}\delta_{ij}]. \tag{59}$$

Thus we only need the component of Q_{33}:

$$Q_{33} = \frac{\pi}{(ef_\pi)^2} \int dx d\theta \sqrt{-g} x^2 (3\cos^2\theta - 1) B^0(x, \theta). \tag{60}$$

The deuteron quadrupole moment is defined as the expectation value of $\hat{Q}_{33}$ with $j_3 = 1$

$$Q = \langle \hat{Q}_{33} \rangle = Q_{33}[\tfrac{3}{2}\langle d, j'_3 = 1 | R^T_{33}(B) R_{33}(B) | d, j_3 = 1\rangle - \tfrac{1}{2}]. \tag{61}$$

Now let us evaluate the matrix element. The rotating matrix R_{33} is represented as $R_{33}(B) = D^1(B)_{00}$ with the Wigner D function. The product of two D functions can be expanded in the following series [14]:

$$D^{J_1}(B)_{M_1N_1} D^{J_2}(B)_{M_2N_2} = \sum_{J=|J_1-J_2|}^{J_1+J_2} \sum_{MN} C^{JM}_{J_1M_1J_2M_2} D^J(B)_{MN} \times C^{JM}_{J_1N_1J_2N_2}. \tag{62}$$

The matrix element of $D^1(B)_{00}$ derived from Eqs. (44) and (45) and the relation of the $D^l(i\tau_2)_{0m} = (-1)^l \delta_{m,0}$,

$$\langle j' j'_3 l'_3 | D^1(B)_{00} | j j_3 l_3 \rangle = -\left(\frac{2j'+1}{2j+1}\right)^{1/2} C^{jl_3}_{j'l'_3 10} C^{jj_3}_{j'j'_3 10}. \tag{63}$$

The deuteron state is the one with $j_3 = 1$. Therefore, inserting $i = 0$, $j = 1$, $\kappa = 0$ and using the constraint in Eq. (36), the matrix element in Eq. (61) is evaluated as

$$Q = -\tfrac{1}{5} Q_{33}. \tag{64}$$

In Fig. 12 α dependence of the Q is shown. As in the case of the magnetic moment, the quadrupole moment significantly decreases with increasing α, which suggests that the D-state probability is strongly affected by the gravity.

The transition moment $\mu_{d\to np}$ for photodisintegration of the deuteron into the isovector $^1S_0$ state is defined by the magnetic moment operator $\hat{\mu}_3$. It is evaluated in terms of the matrix element between the $j_3 = 0$ state and $i_3 = 0$ state:

$$\mu_{d\to np} = \langle ^1S_0, i_3 = 0 | \hat{\mu}_3 | d, j_3 = 0 \rangle. \tag{65}$$

Inserting the dynamical field in Eq. (21) into the isovector part of $\hat{\mu}_i$, one can obtain

$$\hat{\mu}_i|_{I=1} = -\tfrac{1}{2} R_{3j}(A) W_{jk} R_{ki}(B), \tag{66}$$

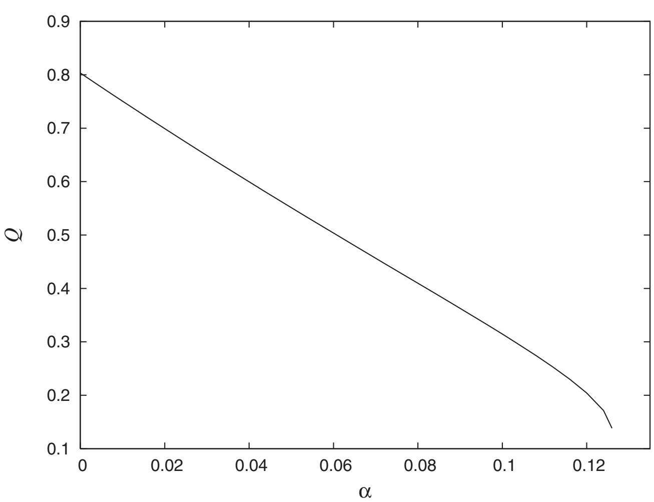

FIG. 12. The coupling constant dependence of the dimensionless quadrupole moment (64).

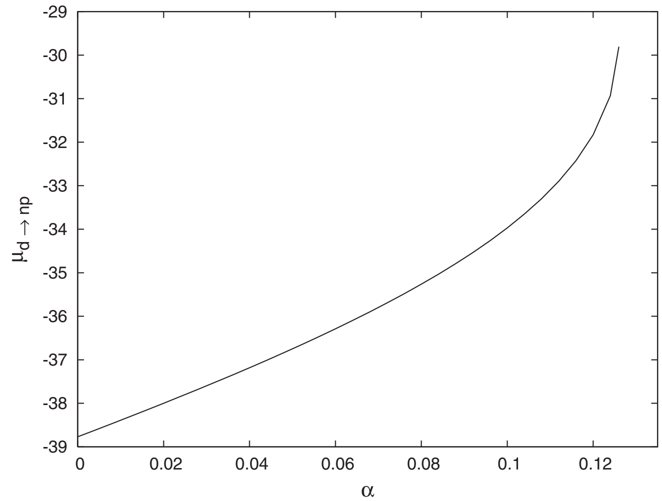

FIG. 13. The coupling constant dependence of the dimensionless transition moment (68).

where W_{jk} is the moment of inertia tensor defined in Eq. (26). From Eq. (32), one can see that W_{33} is the only nonzero component and $W_{33} = 2U_{33}$, and hence

$$\hat{\mu}_3|_{I=0} = -U_{33} R_{33}(A) R_{33}(B). \tag{67}$$

Evaluating the matrix elements of (65) using (63) and the element of the isospace which is derived in the similar way in Eq. (63), one can get

$$\mu_{d\to np} = -\tfrac{1}{3} U_{33}. \tag{68}$$

In Fig. 13 the coupling constant dependence of $\mu_{d\to np}$ is shown. As expected, it also decreases with increasing α. Since the strong gravity reduces the transition moment significantly, it may be possible to determine the gravitational constant by observing the variation in $\mu_{d\to np}$. It is interesting that the decay rates are reduced by the gravitational effects whether the interaction is strong or electromagnetic, which means the gravity works as a stabilizer of baryons.

V. CONCLUSIONS

In this article we have investigated axially symmetric $B = 2$ skyrmions coupled to gravity. Performing collective quantization, we obtained the static observables of the dibaryons. The rotational and isorotational modes were quantized in the same manner as the skyrmion without gravity. It was shown how the static properties of dibaryons such as masses, charge densities, and magnetic moments were modified by the gravitational interaction.

The dependence of the energy density and mean radius on the coupling constant showed that the soliton shrinks as α becomes larger which reflects the attractive feature of gravity. The mass difference between dibaryons also becomes larger as α increases. These observations can be interpreted that shrinking the skyrmion reduces the inertial momenta and hence induces the large mass difference between dibaryon spectra.

In the collective quantization, the skyrmion can be quantized as a slowly rotating rigid body and the various dibaryon spectra are regarded as the rotational bands of the classical skyrmion. Thus the large mass difference means that the gravity works for increasing the rotational kinetic energy of the skyrmion. The magnetic moment is reduced significantly as increasing α compared to that of $B = 1$. We also calculated the quadrupole moment. For the transition moments of the deuteron, we found that the gravity works as a stabilizer. Thus, it may be possible to determine the gravitational constant by the measurement of the various decay rates of the dibaryonic objects.

Throughout the paper, we considered α as a free parameter and studied skyrmion spectra in the strong coupling limit. We found that the effects of gravity on the observables estimated here are manifested only in such a large coupling constant. Some theories such as scalar-tensor gravity theory [15] and theories with extra dimensions discuss the time variation of the gravitational constant [16]. There may have been an epoch in the early universe where the gravitational effects on nucleons were significant.

Let us note that in Ref. [17] the authors computed the quantum correction to the $B = 2$ skyrmion by considering the moduli space of instanton-generated two-skyrmions in the attractive channel which has a larger dimension ($\mathcal{M}_{10}$) than the moduli space of the deuteron ($\mathcal{M}_8$), which greatly improved the deuteron observables. Thus, going beyond the collective coordinate approximation provides a much greater correction to the observables than gravitational effects.

As a future work, the analysis of the electromagnetic form factors of the deuteron is now under consideration. The $SU(3)$ extension and the analysis of dihyperon coupled to gravity will be interesting also.

ACKNOWLEDGMENTS

We would like to thank Rajat K. Bhaduri for drawing our attention to this subject and useful comments.

APPENDIX: FIELD EQUATIONS

For the numerical calculation, we employ the radial coordinate

$$\chi = \frac{x}{1 + x} \tag{A1}$$

to map infinity to $\chi = 1$. The regularity requires the condition

$$m(\chi, 0) = l(\chi, 0). \tag{A2}$$

Following the work of Ref. [9], we introduce the metric function g as

$$g(\chi, \theta) = \frac{m(\chi, \theta)}{l(\chi, \theta)}. \tag{A3}$$

Then the boundary conditions for g are given by

$$g(0, \theta) = 1, \qquad g(\infty, \theta) = 1, \tag{A4}$$

$$g(\chi, 0) = 1, \qquad g\left(\chi, \frac{\pi}{2}\right) = 0. \tag{A5}$$

The filed equations for the profile function $F(\chi, \theta)$ and $\Theta(\chi, \theta)$ are derived as

$$\begin{aligned}
\left(\frac{\delta\sqrt{-g}\mathcal{L}_S}{\delta F}\right)\frac{1}{f_\pi^2}\frac{4}{\sqrt{l}\sin\theta} &= \chi^2(1-\chi)^2\left(F_{,\chi\chi} + \frac{l_{,\chi}}{2l}F_{,\chi}\right) + 2\chi(1-\chi)^2F_{,\chi} + F_{,\theta\theta} + F_{,\theta}\left(\frac{l_{,\theta}}{2l} + \cot\theta\right) \\
&\quad - \{\chi^2(1-\chi)^2\Theta_{,\chi}^2 + \Theta_{,\theta}^2\}\sin F\cos F - \frac{n^2 m}{l\sin^2\theta}\sin F\cos F\sin^2\Theta \\
&\quad + 4\frac{f}{m}\sin^2 F\Big[(1-\chi)^4\Big\{\left(\frac{f_{,\chi}}{f} + \frac{l_{,\chi}}{2l} - \frac{m_{,\chi}}{m}\right)\Theta_{,\theta} - \left(\frac{f_{,\theta}}{f} + \frac{l_{,\theta}}{2l} - \frac{m_{,\theta}}{m} + \cot\theta\right)\Theta_{,\chi} \\
&\quad + \cot F(F_{,\chi}\Theta_{,\theta} - F_{,\theta}\Theta_{,\chi})\Big\}(F_{,\chi}\Theta_{,\theta} - F_{,\theta}\Theta_{,\chi}) + \{\Theta_{,\theta}(F_{,\chi\chi}\Theta_{,\theta} + F_{,\chi}\Theta_{,\chi\theta} - F_{,\chi\theta}\Theta_{,\chi} \\
&\quad - F_{,\theta}\Theta_{,\chi\chi}) - \Theta_{,\chi}(F_{,\chi\theta}\Theta_{,\theta} + F_{,\chi}\Theta_{,\theta\theta} - F_{,\theta\theta}\Theta_{,\chi} - F_{,\theta}\Theta_{,\chi\theta})\} \\
&\quad \times (1-\chi)^4 - 2(1-\chi)^3\Theta_{,\theta}(F_{,\chi}\Theta_{,\theta} - F_{,\theta}\Theta_{,\chi})\Big] \\
&\quad + \frac{4n^2 f}{l\sin^2\theta}\sin^2 F\sin^2\Theta\Big[(1-\chi)^4\Big\{F_{,\chi\chi} + F_{,\chi}^2\cot F + 2F_{,\chi}\Theta_{,\chi}\cot\Theta + \left(\frac{f_{,\chi}}{f} - \frac{l_{,\chi}}{2l}\right)F_{,\chi} \\
&\quad - 2\sin F\cos F\Theta_{,\chi}^2\Big\} - 2(1-\chi)^3F_{,\chi} + \frac{(1-\chi)^2}{\chi^2}\Big\{F_{,\theta\theta} + F_{,\theta}^2\cot F + 2F_{,\theta}\Theta_{,\theta}\cot\Theta \\
&\quad + \left(\frac{f_{,\theta}}{f} - \frac{l_{,\theta}}{2l} - \cot\theta\right)F_{,\theta} - 2\Theta_\theta^2\sin F\cos F\Big\}\Big],
\end{aligned} \tag{A6}$$

$$\left(\frac{\delta\sqrt{-g}\mathcal{L}_S}{\delta\Theta}\right)\frac{1}{f_\pi^2}\frac{4}{\sqrt{l}\sin\theta}\frac{1}{\sin^2F} = \chi^2(1-\chi)^2\left(\Theta_{,\chi\chi}+\frac{l_{,\chi}}{2l}\Theta_{,\chi}\right)+2\chi(1-\chi)^2\Theta_{,\chi}+\Theta_{,\theta\theta}+\Theta_{,\theta}\left(\frac{l_{,\theta}}{2l}+\cot\theta\right)$$
$$+2\{\chi^2(1-\chi)^2F_{,\chi}\Theta_{,\chi}+F_{,\theta}\Theta_{,\theta}\}\cot F-\frac{n^2m}{l\sin^2\theta}\sin\Theta\cos\Theta$$
$$+4\frac{f}{m}\left[(1-\chi)^4\left\{\left(\frac{f_{,\theta}}{f}+\frac{l_{,\theta}}{2l}-\frac{m_{,\theta}}{m}+\cot\theta\right)F_{,\chi}-\left(\frac{f_{,\chi}}{f}+\frac{l_{,\chi}}{2l}-\frac{m_{,\chi}}{m}\right)F_{,\theta}\right\}\right.$$
$$\times(F_{,\chi}\Theta_{,\theta}-F_{,\theta}\Theta_{,\chi})+\{F_{,\chi}(F_{,\chi\theta}\Theta_{,\theta}+F_{,\chi}\Theta_{,\theta\theta}-F_{,\theta\theta}\Theta_{,\chi}-F_{,\theta}\Theta_{,\chi\theta})$$
$$-F_{,\theta}(F_{,\chi\chi}\Theta_{,\theta}+F_{,\chi}\Theta_{,\chi\theta}-F_{,\chi\theta}\Theta_{,\chi}-F_{,\theta}\Theta_{,\chi\chi})\}(1-\chi)^4$$
$$\left.+2(1-\chi)^3F_{,\theta}(F_{,\chi}\Theta_{,\theta}-F_{,\theta}\Theta_{,\chi})\right]$$
$$+\frac{4n^2f}{l\sin^2\theta}\sin^2F\sin^2\Theta\left[(1-\chi)^4\left\{\Theta_{,\chi\chi}+\Theta_{,\chi}^2\cot\Theta+4F_{,\chi}\Theta_{,\chi}\cot F+\left(\frac{f_{,\chi}}{f}-\frac{l_{,\chi}}{2l}\right)\Theta_{,\chi}\right\}\right.$$
$$-2(1-\chi)^3\Theta_{,\chi}+\frac{(1-\chi)^2}{\chi^2}\left\{\Theta_{,\theta\theta}+\Theta_{,\theta}^2\cot\Theta+4F_{,\theta}\Theta_{,\theta}\cot F\right.$$
$$\left.\left.+\left(\frac{f_{,\theta}}{f}-\frac{l_{,\theta}}{2l}-\cot\theta\right)\Theta_{,\theta}\right\}\right]-\frac{4n^2f}{l\sin^2\theta}\sin\Theta\cos\Theta\left[(1-\chi)^4F_{,\chi}^2+\frac{(1-\chi)^2}{\chi^2}F_{,\theta}^2\right]. \quad \text{(A7)}$$

From Einstein equations, the field equations for the metric functions are derived. We diagonalized those equations to the 2nd derivative of χ and θ for each metric function

$$\frac{m}{f^2}x^2G_{00}+x^2G_{11}+G_{22}+\frac{m}{l\sin^2\theta}G_{33}-2\alpha\left[\frac{m}{f^2}\hat{r}^2T_{00}+\hat{r}^2T_{11}+T_{22}+\frac{m}{l\sin^2\theta}T_{33}\right]$$
$$=\chi^2(1-\chi)^2\frac{f_{,\chi\chi}}{f}-\chi^2(1-\chi)^2\left(\frac{f_{,\chi}}{f}\right)^2+2\chi(1-\chi)^2\frac{f_{,\chi}}{f}+\frac{f_{,\theta\theta}}{f}-\left(\frac{f_{,\theta}}{f}\right)^2+\cot\theta\frac{f_{,\theta}}{f}+\frac{1}{2}\chi^2(1-\chi)^2\frac{f_{,\chi}}{f}\frac{l_{,\chi}}{l}$$
$$+\frac{1}{2}\frac{f_{,\theta}}{f}\frac{l_{,\theta}}{l}-\alpha\left[2\frac{f}{m}(1-\chi)^4(F_{,\chi}\Theta_{,\theta}-F_{,\theta}\Theta_{,\chi})^2\sin^2F+\frac{2n^2f}{l\sin^2\theta}\left\{(1-\chi)^4(F_{,\chi}^2+\Theta_{,\chi}^2\sin^2F)\right.\right.$$
$$\left.\left.+\frac{(1-\chi)^2}{4\chi^2}(F_{,\theta}^2+\Theta_{,\theta}^2\sin^2F)\right\}\sin^2F\sin^2\Theta\right], \quad \text{(A8)}$$

$$\frac{m}{l\sin^2\theta}G_{33}-2\alpha\left[\frac{m}{l\sin^2\theta}T_{33}\right]=\frac{1}{2}\chi^2(1-\chi)^2\frac{m_{,\chi\chi}}{m}+\frac{1}{2}\chi(1-\chi)(1-2\chi)\frac{m_{,\chi}}{m}-\frac{1}{2}\chi^2(1-\chi)^2\left(\frac{m_{,\chi}}{m}\right)^2+\frac{1}{2}\frac{m_{,\theta\theta}}{m}$$
$$-\frac{1}{2}\left(\frac{m_{,\theta}}{m}\right)^2+\frac{1}{4}\chi^2(1-\chi)^2\left(\frac{f_{,\chi}}{f}\right)^2+\frac{1}{4}\left(\frac{f_{,\theta}}{f}\right)^2+\frac{\alpha}{4}\left[\chi^2(1-\chi)^2(F_{,\chi}^2+\Theta_{,\chi}^2\sin^2F)\right.$$
$$+F_{,\theta}^2+\Theta_{,\theta}^2\sin^2F-\frac{n^2m}{l\sin^2\theta}\sin^2F\sin^2\Theta+4\frac{f}{m}(1-\chi)^4(F_{,\chi}\Theta_{,\theta}-F_{,\theta}\Theta_{,\chi})^2\sin^2F$$
$$\left.-\frac{4n^2f}{l\sin^2\theta}\sin^2F\sin^2\Theta\left\{(1-\chi)^4(F_{,\chi}^2+\Theta_{,\chi}^2\sin^2F)+\frac{(1-\chi)^2}{\chi^2}(F_{,\theta}^2+\Theta_{,\theta}^2\sin^2F)\right\}\right], \quad \text{(A9)}$$

$$x^2G_{11}+G_{22}-2\alpha[x^2T_{11}+T_{22}]=\frac{1}{2}\chi^2(1-\chi)^2\frac{l_{,\chi\chi}}{l}-\frac{1}{4}\chi^2(1-\chi)^2\left(\frac{l_{,\chi}}{l}\right)^2+\chi(1-\chi)\left(\frac{3}{2}-\chi\right)\frac{l_{,\chi}}{l}+\frac{1}{2}\frac{l_{,\theta\theta}}{l}-\frac{1}{4}\left(\frac{l_{,\theta}}{l}\right)^2$$
$$+\cot\theta\frac{l_{,\theta}}{l}-\alpha\left[2\frac{f}{m}(1-\chi)^4(F_{,\chi}\Theta_{,\theta}-F_{,\theta}\Theta_{,\chi})^2\sin^2F-\frac{n^2m}{2l\sin^2\theta}\sin^2F\sin^2\Theta\right]. \quad \text{(A10)}$$

[1] T. H. R. Skyrme, Proc. R. Soc. A **260**, 127 (1961).
[2] G. S. Adkins, C. R. Nappi, and E. Witten, Nucl. Phys. **B228**, 552 (1983).
[3] N. S. Manton, Phys. Lett. B **192**, 177 (1987).
[4] V. B. Kopeliovich and B. E. Stern, Pis'ma Zh. Eksp. Teor. Fiz..**45**, 165 (1987) [JETP Lett. **45**, 203 (1987)].
[5] J. J. M. Verbaarschot, Phys. Lett. B **195**, 235 (1987).
[6] E. Braaten and L. Carson, Phys. Rev. D **38**, 3525 (1988).
[7] H. Luckock and I. Moss, Phys. Lett. B **176**, 341 (1986).
[8] N. Sawado, N. Shiiki, K. Maeda, and T. Torii, Gen. Relativ. Gravit. **36**, 1361 (2004).
[9] T. Ioannidou, B. Kleihaus, and W. Zakrzewski, Phys. Lett. B **600**, 116 (2004).
[10] N. Shiiki, N. Sawado, and S. Oryu, Phys. Rev. D **70**, 114023 (2004).
[11] B. Kleihaus and J. Kunz, Phys. Rev. Lett. **79**, 1595 (1997).
[12] D. Finkelstein and J. Rubinstein, J. Math. Phys. (N.Y.) **9**, 1762 (1968).
[13] A. De Rujula, H. Georgi, and S. L. Glashow, Phys. Rev. D **12**, 147 (1975).
[14] D. A. Varshalovich, A. N. Moskalev, and V. K. Khersonskii, *Quantum Theory of Angular Momentum* (World Scientific, Singapore, 1988).
[15] C. Brans and R. H. Dicke, Phys. Rev. **124**, 925 (1961).
[16] W. J. Marciano, Phys. Rev. Lett. **52**, 489 (1984).
[17] R. A. Leese, N. S. Manton, and B. J. Schroers, Nucl. Phys. **B442**, 228 (1995).